E. L. Gruenberg
H. P. Raabe
C. T. Tsitsera

Self-directional Microwave Communication System

Abstract: This paper describes a communication system in which sending and receiving terminals automatically generate beams focused upon each other, which arise solely from ambient noise. The terminals are amplifying retrodirective arrays of antenna elements. Analysis and experiment are used to prove and verify the system concept. Some engineering considerations pertinent to system operation under various conditions are also analyzed and discussed.

Introduction

The use of directional (as contrasted with omnidirectional) transmission for wireless communication reduces the required amount of the radio frequency (rf) power and the possibility of interference between users. When microwave carrier signals are used, higher directivity can be attained because large aperture-to-wave-length ratios can be achieved with antennas of reasonable size.

In many applications the locations of transmitting and receiving terminals are unknown or varying with respect to each other; hence, the capability for varying the direction of transmission must be available. This has been achieved in the past by either mechanical or electronic steering of the signal beam. Initial signal acquisition is generally established by a process in which one terminal scans its field of view to locate the source of an omnidirectional pilot signal transmitted by another terminal. In recent years considerable research and development effort has been expended in studying methods for achieving directional communications. (See, for example, the collection of papers in Ref. [1].)

This paper describes a communication system capable of providing directional transmission and reception between terminals of unknown position without requiring prior scanning on the part of either terminal; i.e., the system is self-directional. The system concept is novel in the use of retrodirective antenna arrays to generate beams originating at the transmitting and receiving arrays, focused upon each other, which arise solely from ambient noise radiated by the arrays. As the arbitrarily low-level noise is radiated from one terminal and reflected back to it, with the full array gain of the opposite terminal, an oscillating signal is built up. After a sufficient number of round trips between terminals, this signal becomes a carrier that can be modulated, with the result that directional communication between the two terminals becomes possible [2].

The main purpose of this paper is to prove through analysis and experiment that there will be a build up of a carrier into a focused beam between two retrodirective arrays. The basic analytical result is the power spectral density of the signal during the build-up period. Besides this result, which is important in proving the feasibility of the system concept, certain engineering considerations are discussed. Methods of frequency conversion that permit transmitting and receiving at different frequencies have a significant impact on the system characteristics and are analyzed.

System concept

The generation of feedback oscillation between two terminals for the purpose of communication has been proposed by Espenschied [3]. This process of building an oscillating carrier starting from noise has been referred to as "singing." The singing loops considered by Espenschied use omnidirectional antennas or mechanically pointed directional antennas.

For the system considered in the present paper, the retrodirective properties of arrays are essential to the

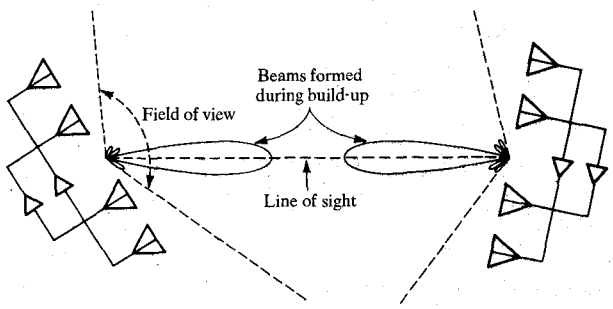

Figure 1 Two amplifying Van Atta arrays generating beamed retrodirective radiation.

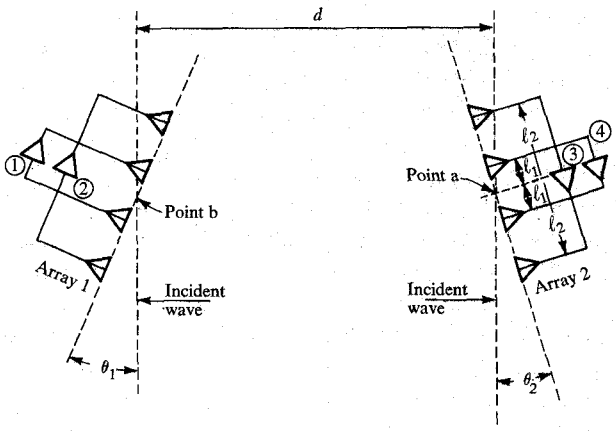

Figure 2 Geometry of retrodirective arrays.

directional focusing of the beams. In 1959 L. C. Van Atta received a patent for a passive retrodirective phased array [4]. He showed that if the transmitter is in the field of view of a planar array of antenna elements appropriately connected by lines of equal electrical length, a plane wave of energy incident on the array would be reflected back in the direction of the source. The retrodirective gain of a Van Atta array may be increased by the insertion of amplifiers in the interconnecting transmission lines, although the achievable gain is limited by the electromagnetic isolation between receiving and transmitting array elements. Nonetheless, two amplifying Van Atta arrays form the basic configuration of the self-directional communication system as illustrated in Fig. 1.

When the two retrodirective arrays (which are within each other's field of view) are turned on, there is a noise output from each antenna element due to thermal and other external noise sources. Because the sources are independent, the thermal component of output noise is radiated throughout the entire field of view of the array. Part of this noise output is received by the opposite array, but at a much lower power level than the noise generated locally in the receiving array. However, the received noise is coherent across the receiving aperture. Because the system is linear at low power levels, the noise received from the opposite array is returned in the direction from which it was received with the full gain of the array. Thus, perhaps contrary to intuition, the noise present in the amplifiers does not overwhelm the incident low-level radiation and frustrate the build-up of a focused beam. The build-up process continues until it is limited by the power capability of the transmitting elements or by a limiter located in the system.

The electronic gain in each terminal can be increased (as required for communication between terminals separated by a long distance) if the received signal is subjected to frequency translation before retransmission. For large arrays and large differences between receiving and transmitting frequencies, the receiving and transmitting elements in each terminal must be divided into sets of separate arrays scaled for wavelength. It is possible to use circulators so that all elements of a terminal can be used for both reception and transmission if the two frequencies do not differ greatly.

The retrodirective property required for the system to operate as intended can also be obtained with phase inversion of the signals before retransmission. Such a scheme permits the signal received at each element to be retransmitted from the same element and allows the use of conformal arrays [5].

In all variations of this system concept, as in any delay oscillator, there is a multiplicity of possible modes of oscillation. The selection of one of these modes occurs through filtering and amplitude-limiting in the loop. The several ways available for frequency translation in the two terminals have different effects on the types of possible modes and on which of the several modes is selected. These effects are considered after analysis of the oscillation build-up.

Analysis of carrier build-up

We wish to prove that two retrodirective arrays oriented so that they are within each other's field of view will sing, i.e., that an oscillating signal will build up between the arrays, with the full gain of the antenna arrays, from noise inputs. It is important to know how long, starting from a given background noise level, it takes for the oscillations to reach a specified, higher power level. From the following analysis, the relationship between build-up time, power level, array separation, and antenna characteristics can be obtained. In addition, the analysis gives the power spectral density as a function of time during the linear portion of the build-up, i.e., before limiting occurs in the system.

Figure 2 shows diagrams of two retrodirective arrays, where for simplicity each array is depicted with two receiving and two transmitting elements. The thermal noise input to the amplifier of each element is assumed to be narrow-band white noise and to be independent of all other noise inputs. Each antenna element is treated as if it were independent of every other element; mutual coupling is neglected.

The autocorrelation of the input to one of the amplifiers is derived. Although this autocorrelation varies with time, intervals exist during which it is independent of time. In these intervals, the power spectral density can be obtained by taking the Fourier transform of the autocorrelation function.

The thermally generated noise output of each antenna element in Array 1 produces a field at Array 2 at the point labeled a in Fig. 2. It is assumed that the arrays are sufficiently far apart that incident wavefronts can be treated as planar. The total field at a is the sum of fields produced by the independent sources of Array 1. This field at a, combined with the locally generated thermal noise, produces, in turn, a voltage at the input to each amplifier in Array 2.

In the Appendix the autocorrelation function and the power spectral density of the input to a typical amplifier are derived for the process described above. This input [designated as $y(t)$] has a time-varying autocorrelation function that is, however, independent of time in the intervals $nt_d + (2/B)$ to $(n+1)\,t_d$, where t_d is the one-way transit time, and B is the bandwidth of the terminal. During the time-independent intervals, the autocorrelation function of $y(t)$ is given, for even values of n, by

$$R_{yy}(\tau) = R(\tau) + \frac{1}{N}\sum_{j=1}^{n/2} A^{2j}[R(\tau + 2jt_d) + R(\tau - 2jt_d)] + \frac{1}{N}\sum_{k=1}^{n/2} A^{2k}\sum_{j=1}^{n/2} A^{2j}R[\tau + 2(k-j)t_d] + \frac{1}{N}\sum_{k=0}^{(n/2)-1} A^{2k+1}\sum_{j=0}^{(n/2)-1} A^{2j+1}R[\tau + 2(k-j)t_d], \quad (1)$$

where A is the one-way voltage gain of the loop (including coherent excitation of the array), N is the number of array elements, and $R(\tau)$ is the autocorrelation function of narrow-band noise.

Except during short intervals following each multiple of the transit time, the process can be treated as stationary and the power spectral density can be computed from the Fourier transform of the autocorrelation function (1). Examination of the power spectral density for various values of A and N allows one to see how the spectrum changes during the build-up period before limiting occurs in the system. The power spectral density of $y(t)$ during the stationary intervals, as derived in the Appendix, is given by

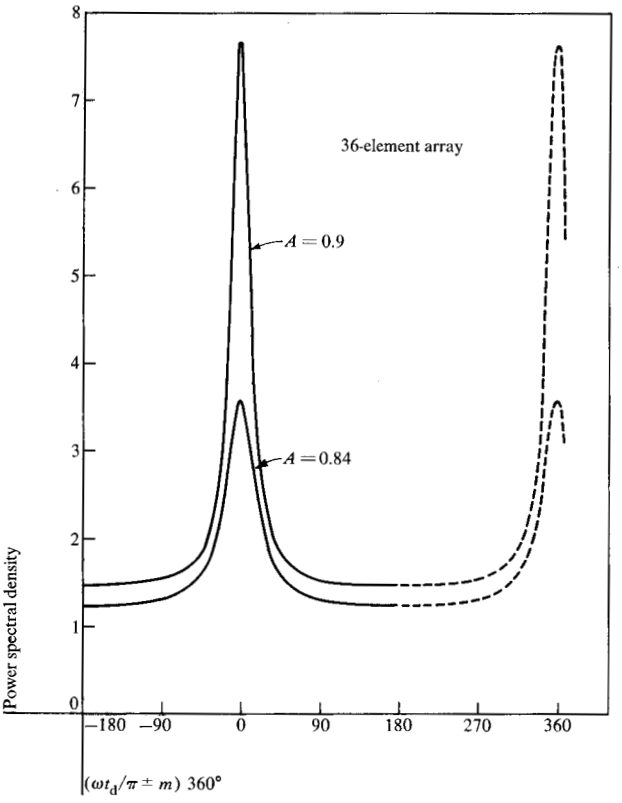

Figure 3 Steady state power spectral density of one mode for A < 1, normalized to $S(\omega)$.

$$S_n(\omega)/S(\omega) = 1 + \{A^2[1 - A^2 + A^4 - A^{2n+4} + (1 - 2A^2 + A^{2n+2})\cos 2\omega t_d] + A^{n+2}(A^2 - 1)[\cos n\omega t_d + \cos(n+2)\omega t_d]\} \div N(1 - A^2)(1 + A^4 - 2A^2\cos 2\omega t_d). \quad (2)$$

where $S(\omega)$ is the power spectrum of narrow-band noise.

It can be noted that the power spectral density diverges with n if the one-way voltage gain A is equal to or greater than 1 and converges if A is less than 1. For large n, and A less than 1,

$$\lim_{n\to\infty}\frac{S_n(\omega)}{S(\omega)} = 1 + \frac{A^2(1 - A^2 + A^4) + A^2(1 - 2A^2)\cos 2\omega t_d}{N(1 - A^2)(1 + A^4 - 2A^2\cos 2\omega t_d)}. \quad (3)$$

This limit is plotted as a function of ωt_d for two values of A and for $N = 36$ in Fig. 3. The function is periodic in $2\omega t_d$, with peaks of the power spectral density occurring when

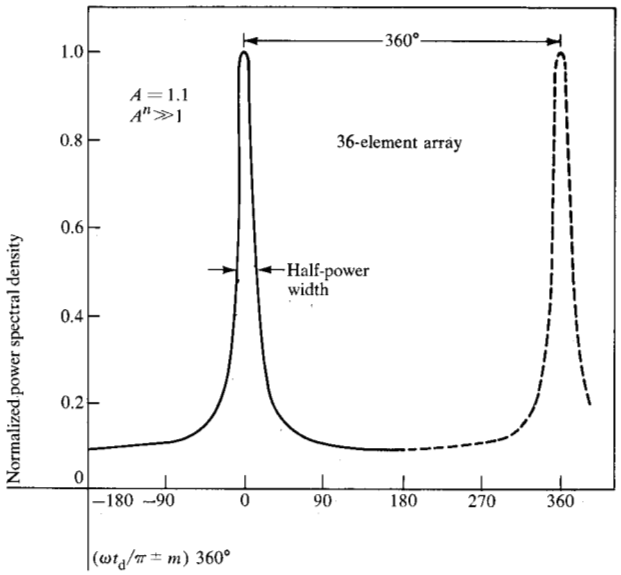

Figure 4 Normalized power spectral density of one mode for $A > 1$.

$$2\omega t_d = m(2\pi),\ m = 0, 1, 2, \cdots \tag{4}$$

or, equivalently, when

$$f = \frac{m}{2t_d} = \frac{m}{2}\left(\frac{d}{c} + t_a\right)^{-1}, \tag{5}$$

where the signal frequency f is in the passband of the system, d is the distance between points a and b of Fig. 2, c is the speed of propagation, and t_a is the internal delay of one array. Each integer value of m gives a different mode frequency, and $m = 1$ gives the basic mode.

If A is greater than 1 and n is large, Eq. (2) reduces to

$$\frac{S_n(\omega)}{S(\omega)} = 1 + \frac{A^{2n+4}}{N(A^2 - 1)}\left[\frac{A^2 - \cos 2\omega t_d}{1 + A^4 - 2A^2 \cos 2\omega t_d}\right]. \tag{6}$$

The normalized power spectrum for one of the modes in the frequency passband is shown in Fig. 4 for $A = 1.1$ for $A^n \gg 1$. The normalized spectrum is independent of n and of time as long as $A^n \gg 1$. Of course, the power spectrum actually increases in magnitude as can be seen from Eq. (6). The shape of the spectrum does not change,

Figure 5 Peak power density vs the number n of one-way trips, normalized to $S(\omega)$.

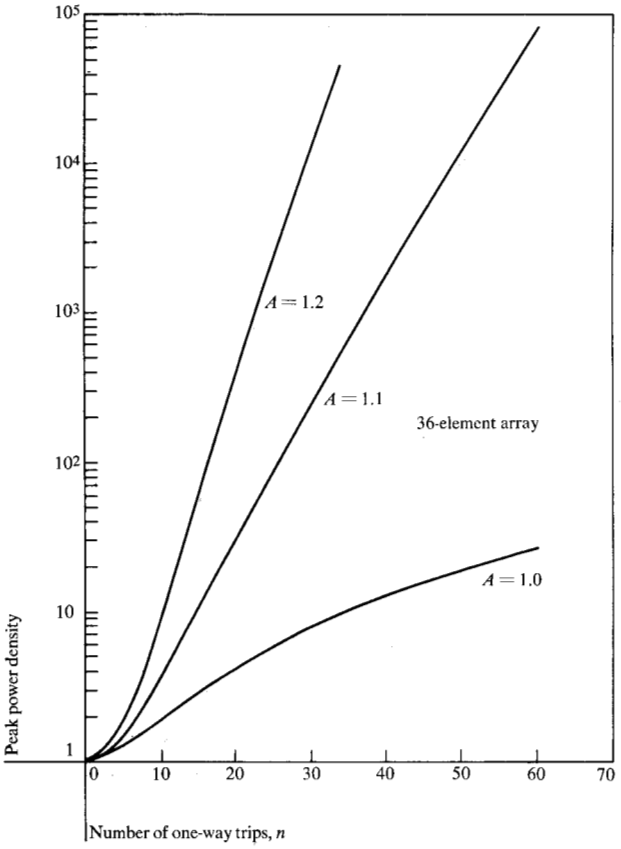

Figure 6 Total power in passband vs number n of one-way trips, normalized to total initial power.

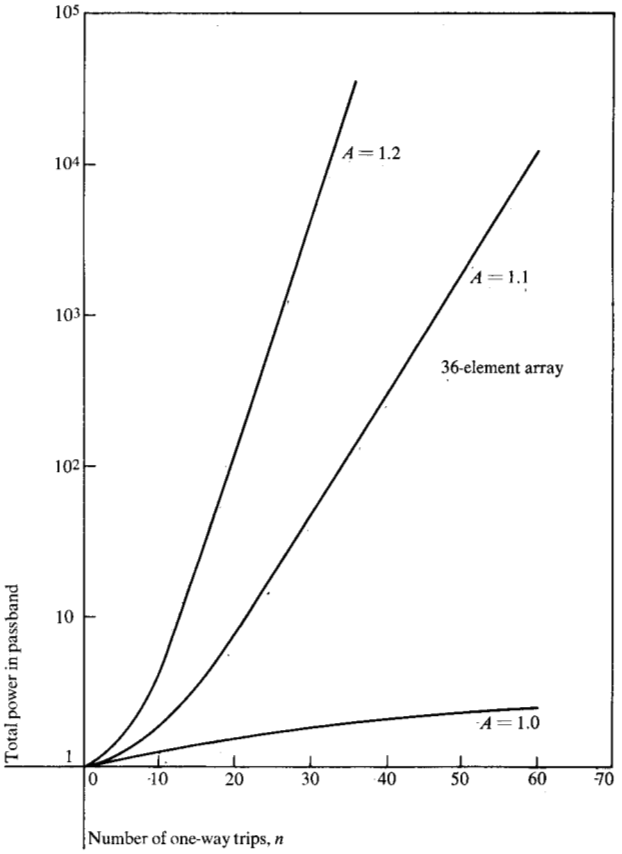

however, while operation is restrained to the linear portion of the amplifiers. When limiting occurs, the spectrum changes, as is discussed later. Since $S(\omega)$ is a constant, S_0, in the passband, the peak value of the spectrum occurs when ωt_d is a multiple of 2π. From Eq. (2) one obtains

$$\frac{S_n\left(\frac{2\pi m}{t_d}\right)}{S_0} = \begin{cases} 1 + \dfrac{A^2(2 - A^2 - 2A^n + A^{2n+2})}{N(1 - A^2)^2} \\ \quad \text{for } A \neq 1; \\ 1 + \dfrac{1}{N}\left(\dfrac{n^2}{4} + n\right) \text{ for } A = 1. \end{cases} \tag{7}$$

The peak power density is plotted in Fig. 5 as a function of the number of one-way trips for $A = 1$, 1.1, and 1.2.

The average power in the passband can be obtained by integrating Eq. (2) over all frequencies:

$$P_{\text{avg}} = \begin{cases} \left[1 + \dfrac{A^2}{N}\left(\dfrac{1 - A^{2n}}{1 - A^2}\right)\right] 2BS_0 \text{ for } A \neq 1; \\ \left(1 + \dfrac{n}{N}\right) 2BS_0 \text{ for } A = 1. \end{cases} \tag{8}$$

The normalized total power in the passband is plotted in Fig. 6 for $A = 1$, 1.1, and 1.2.

The time to build up the peak of the spectrum to a given value can be obtained from Eq. (7). The number of one-way trips to build up the spectrum peak to PS_0 is given approximately by

$$n = \tfrac{1}{2}\log[(P - 1)N(A^2 - 1)^2 A^{-4}](\log A)^{-1} \text{ for } A^n > 1. \tag{9}$$

Since n is equal to t/t_d, the build-up time is given by

$$t = n\left(\frac{d}{c} + t_a\right). \tag{10}$$

Figure 7 shows the number of one-way trips in the loop required for the peak spectrum power in each amplifier input to reach 100 times the noise spectral density S_0. The function is plotted against the one-way voltage gain A and the equivalent gain in dB. Figure 7 shows that the time to build up to a useful spectral value is strongly dependent on the one-way gain and weakly dependent on the number of array elements. A 1-dB increase in gain above zero dB reduces the build-up time by a factor of about four. A 1000-element array requires only approximately twice the build-up time of a 36-element array.

When the oscillation builds up to the point that saturation or limiting occurs in the system, the spectrum changes. Because of the nonuniform gain characteristics of the filters in the system, some of the modes receive a higher gain than others and build up at a faster rate. The combination of amplitude-limiting and filtering results, in most circumstances, in the selection of one of these modes and the suppression of the others. This effect is considered in some detail by Edson [6] for multi-mode oscillators. As Edson points out, the frequencies in a

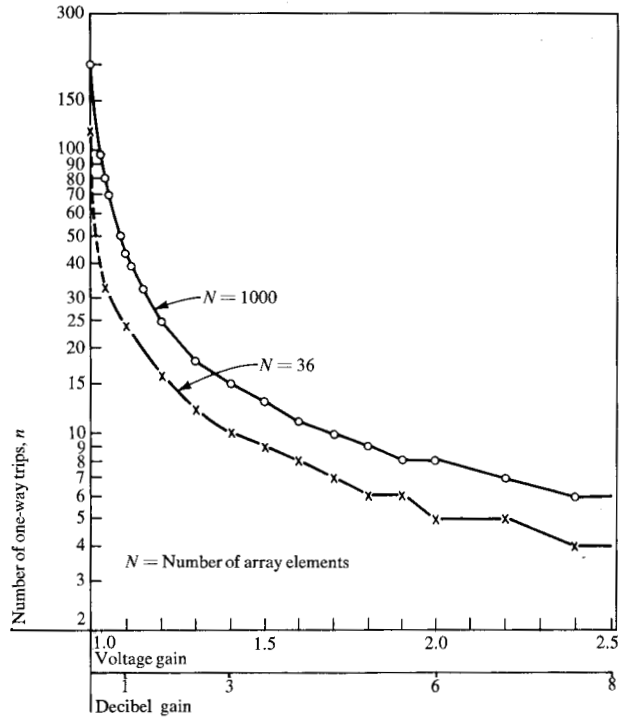

Figure 7 Number of one-way trips required for the peak power in each amplifier to reach 100 S_0 as a function of one-way voltage gain A.

delay-type system are separated by constant increments, so that small-deviation phase modulation that is not affected by amplitude-limiting and filtering results. If the gain characteristics of the filters are ripple-free so that they are concave downward, this phenomenon will generally be avoided.

As discussed in the next section, one of the two-frequency systems (the single-inversion system) has modes that are related in a way such that they constitute amplitude modulation. Amplitude-limiting and filtering remove the amplitude modulation, leaving the one mode, which can be used as the carrier.

Two-frequency systems

The analysis presented so far has been for the spectral build-up of a monofrequency singing loop; that is, a system in which no frequency conversion is used. However, practical reasons exist for such conversion, one of which is to provide isolation between receiver and transmitter. Another reason, intermediate frequency (if) amplification, is discussed later.

The simplest type of two-frequency system possible is shown in Fig. 8 and includes two local oscillators to produce frequency offset. The system can be operated in three different ways, depending on the choice of local oscillator and filter frequencies. Assume there is up-

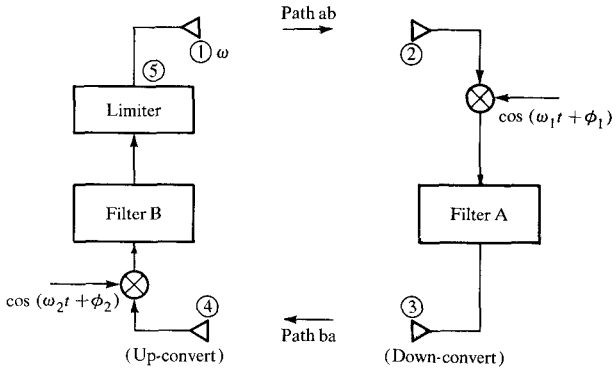

Figure 8 Schematic of simple two-frequency system.

conversion in the left unit and down-conversion in the right unit. In each unit the conversion can be achieved simply by shifting the received signal frequency or by inverting the signal frequency.

Since there are two possible ways of frequency conversion in each of the two terminals, there are four possible schemes, the following three of which have essential differences: 1) shifting in both terminals, 2) inversion in both terminals, and 3) shifting in one terminal and inversion in the other.

In each case, assume that the signal at Point 1 is given by

$$x(t) = \cos(\omega t + \phi). \tag{11}$$

For a steady state solution to exist, the signal that results after each transit around the loop must be identical to the transmitted signal. Thus, for frequency shifting or phase inversion in both terminals,

$$\cos[(\omega_2 - \omega_1 + \omega)t + (\omega_1 - 2\omega)t_d + \phi - \phi_1 + \phi_2] = \cos(\omega t + \phi), \tag{12}$$

and for inversion down in one terminal and shifting up in the other,

$$\cos[(\omega_2 + \omega_1 - \omega)t + (2\omega - \omega_1)t_d - \phi + \phi_1 + \phi_2] = \cos(\omega t + \phi). \tag{13}$$

In order that these equations hold for all time, the conditions listed in Table 1 must exist. Thus, for double shifting or double inversion, as in the monofrequency system, there is a multiplicity of possible frequencies or modes, mutually separated by the frequency $1/2t_d$. The selection of one of the modes depends upon the combination of filtering and amplitude-limiting. Note that since the oscillation frequency depends upon the loop time delay and the phases of the local oscillation, the filter bandwidths must be wider than the spacing between modes to ensure that build-up will occur.

For double shifting or double inversion, the local oscillators must be in synchronism to enable the carrier frequency ω to remain constant. Otherwise, the carrier will gradually shift through the passband, the loop gain will become less than one, and the oscillation will decay. As the old mode decays, the loop gain in the center of the amplifier passband increases and the nearest mode builds up to the limiting level. This mode will also shift toward the edge of the passband and decay, so that repetitive mode switching will result, rendering the carrier useless for undisturbed transmission of a modulated signal. To achieve a stable mode, one of the local oscillators must

Table 1 Frequency-phase relationships.

Case	*Requirements for local oscillators*	*Resulting frequency at Point 1*	*Resulting phase at Point 1*
Shifting in both terminals	$\omega_2 = \omega_1$	$\omega = \frac{\phi_2 - \phi_1}{2t_d} \pm \frac{m\pi}{t_d} + \frac{\omega_1}{2}$ $m = 0, 1, 2, \cdots$	Any
Inversion in both terminals	$\omega_2 = \omega_1$	$\omega = \frac{\phi_2 - \phi_1}{2t_d} \pm \frac{m\pi}{t_d} + \frac{\omega_1}{2}$ $m = 0, 1, 2, \cdots$	Any
Inversion down and shift up	None	$\omega = \frac{\omega_2 + \omega_1}{2}$	$\phi = \frac{\phi_1 + \phi_2}{2} + \frac{\omega_2 t_d}{2}$ $\pm m\pi$

be voltage-controllable. The control voltage can be derived from a frequency discriminator that monitors the transmitted frequency [5].

The double-shift and double-inversion systems appear identical (see Table 1). However, there is an important difference when the effect of relative motion of the two terminals is considered, as is shown later.

The characteristics of a system with one inversion and one shift are quite different from those of the other two systems. No synchronization of the local oscillators is required. The frequency of oscillation is determined by the two local oscillator frequencies and is independent of the distance between the two terminals. The oscillation occurs at a specific phase, which depends on the distances and the phases of the local oscillators. There is also a multiplicity of modes in this system, but they are dependent on one another. These modes occur because a signal that passes through the system twice returns to the source at its original frequency. However, if the signal is also to return at the same phase, the following restrictions on the frequency are necessary:

$$\omega = \frac{\omega_1 + \omega_2}{2} \pm \frac{k\pi}{2t_d}, \qquad k = 0, 1, 2, \cdots. \tag{14}$$

The phases of these modes are related to the phase of the main mode in such a manner that the result is an amplitude-modulated wave. For example, consider a case in which the passband of the filter is wide enough to support only three modes. We would have

$$\begin{aligned} x(t) = {} & \cos\left[\left(\frac{\omega_1 + \omega_2}{2}\right)t + \phi\right] \\ & + b\cos\left[\left(\frac{\omega_1 + \omega_2}{2} + \frac{\pi}{2t_d}\right)t + \phi_3\right] \\ & + b\cos\left[\left(\frac{\omega_1 + \omega_2}{2} - \frac{\pi}{2t_d}\right)t - \phi_3 + 2\phi\right], \end{aligned} \tag{15}$$

where the phase ϕ is as given in Table 1 and ϕ_3 is independent of ϕ, and it has been assumed that the main mode is of unit amplitude, whereas the others are of amplitude b.

These two modes are spaced $\pm\, 1/4t_d$ Hz with respect to the main one. They cannot exist independently of each other. Equation (15) can be expressed as

$$\begin{aligned} x(t) = {} & \left[1 + 2b\cos\left(\frac{\pi}{2t_d}t + \phi_3\right)\right] \\ & \times \left[\cos\left(\frac{\omega_1 + \omega_2}{2}\right)t + \phi\right], \end{aligned} \tag{16}$$

showing that these modes produce amplitude modulation. For this reason, all modes except the main mode (the carrier) should be eliminated rapidly by the limiter.

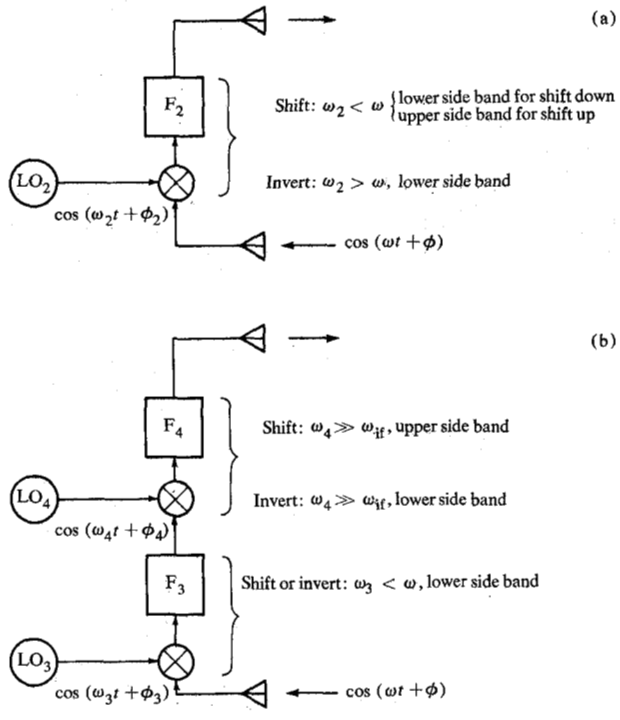

Figure 9 Comparison of terminals using (a) rf and (b) if amplification.

In the single-shift, single-inversion system it can be shown that the effective amplification for the main mode is larger than that for any of the other modes, as long as the filter characteristics are concave. This characteristic behavior is true even with errors in local oscillator frequencies; it results from the fact that a mode frequency offset by $\pm\,\Delta$ with respect to the main mode returns after one round trip offset by $\mp\,\Delta$. The higher effective amplification of the main mode, along with the fact that the resultant signal is amplitude-modulated, causes the limiting action to be more effective in suppressing all but the main mode.

Systems using if amplification

There are two main reasons for using if amplification in the terminals. First, it is generally less expensive to provide the required electronic amplification at if than it is at rf. Second, the narrow-band filtering that may be required to limit the transmitted power for the carrier and to limit the number of possible modes of oscillation is more conveniently provided at intermediate frequencies.

Figure 9 compares if and rf amplifying terminals. The restrictions on the local oscillator frequencies shown in Fig. 9 allow shifting or inverting terminals to be used, with the lowest possible oscillator frequencies. The frequency of the first local oscillator (LO_3) which is used to down-convert the incoming signal, can always be lower

than that of the incoming signal. The second conversion determines whether the terminal is shifting or inverting.

Since, from a receiving and transmitting point of view, these are two terminal devices, the equivalence of the if and rf amplifying devices can be derived. The previously derived equations for loops using rf amplification apply as well to loops with if amplification if the substitutions shown in Table 2 are made.

Systems using if amplification are considered in more detail in Fig. 10. Four cases are considered. Since one terminal must have a resulting up-conversion of frequency and the other a down-conversion, the four cases cover all possible situations.

The resultant link frequencies are given in terms of the local oscillator frequencies. For specified link frequencies $\omega_{\rightarrow}$ and $\omega_{\leftarrow}$ and specified if frequencies, the local oscillator frequencies are given. It is assumed that the same if frequency is used in each terminal.

Note that for cases 1 and 2, the shift-shift and invert-invert cases, respectively, a frequency discriminator and voltage control of one of the oscillators are necessary in order to achieve the relations between frequencies required for stable oscillation. Note also that as in the rf amplifying cases considered previously, the modes are separated by π/t_d radians per second. The frequency $\omega_{\rightarrow}$, which is the link frequency from the left to the right terminal, depends on the filter and limiter characteristics.

As noted in Table 1, the absolute values of the mode frequencies depend upon the phase relationship between local oscillators through the expression $(\phi_2 - \phi_1)/2t_d$. Because the phases can differ by any value in the range $\pm\pi$, the absolute frequencies of the modes can differ by as much as $\pm\pi/2t_d$ radians per second. This difference covers the entire frequency separation of the modes, π/t_d.

It can also be seen in Fig. 10 that for the shift-shift case, the local oscillators determine the difference between the two link frequencies, i.e., $\omega_{\leftarrow} - \omega_{\rightarrow} = \omega_3 - \omega_4$. In the invert-invert case the local oscillators directly determine the sum of the two link frequencies; i.e., $\omega_{\leftarrow} + \omega_{\rightarrow} = \omega_3 + \omega_4$.

The most attractive cases are shift-up, invert-down and shift-down, invert-up (cases 3 and 4, respectively). Their attractiveness is due to the fact that there is no requirement on the absolute values of oscillator frequencies. A carrier will be built up even if one of the frequencies differs significantly from its nominal value, provided that the loop bandwidth is sufficiently wide.

Table 2 Equivalence of rf and if terminals.

Terminal type	*Substitute for* ω_2	*Substitute for* ϕ_2
Shift up	$\omega_4 - \omega_3$	$\phi_4 - \phi_3$
Shift down	$\omega_3 - \omega_4$	$\phi_3 - \phi_4$
Invert up	$\omega_3 + \omega_4$	$\phi_3 + \phi_4$
Invert down	$\omega_3 + \omega_4$	$\phi_3 + \phi_4$

The required loop bandwidth can be determined by considering the changes in if frequencies resulting from oscillator frequency errors. Assume that the two local oscillator frequencies in each terminal are synthesized from the same source and, therefore, have the same percent error. Given the errors δ_1 and δ_2 for the left and right terminals, respectively, the changes in if frequencies for case 3 are

$$\Delta(\omega_{if})_{left} = -\delta_1\left(\frac{\omega_3 + \omega_4}{2}\right) + \delta_2\left(\frac{\omega_6 + \omega_5}{2}\right)$$

and

$$\Delta(\omega_{if})_{right} = \delta_1\left(\frac{\omega_4 - \omega_3}{2}\right) + \delta_2\left(\frac{\omega_6 - \omega_5}{2}\right).$$

As an example, consider a shift-up, invert-down system (case 3) with $f_{\rightarrow} = 1000$ MHz, $f_{\leftarrow} = 940$ MHz, $f_{if} = 70$ MHz, and $\delta_1 = \delta_2 = \pm 10^{-6}$. Then, from Table 2, $f_3 = 870$ MHz, $f_4 = 930$ MHz, $f_5 = 930$ MHz, and $f_6 = 1010$ MHz. The required minimum carrier bandwidths calculated from the above relations are $\pi^{-1}\Delta(\omega_{if})_{left} = 3740$ Hz and $\pi^{-1}\Delta(\omega_{if})_{right} = 140$ Hz.

Effect of terminal motion

Relative motion of the terminals affects the oscillation. In the single-inversion system a stable frequency of oscillation will occur. Although the frequency of this oscillation is dependent upon motion and local oscillator signals, there is no need to adjust the local oscillator frequency to obtain an oscillation. This is a significant difference from the other two systems.

The differences in performance of the three systems when relative motion exists between the terminals can be seen by assuming again that a signal $x(t) = \cos(\omega t + \phi)$ is transmitted from Point 1 shown in Fig. 8. Assume that the left terminal is fixed and the right terminal is moving radially away from it with a velocity v. The signal received at Point 1 after traveling around the loop and experiencing the frequency conversions and Doppler shifts in the outgoing and incoming links must have frequency and phase equal to those of the transmitted signal. It can be shown that the following requirements exist:

$$\omega = \frac{\omega_1 + \omega_2}{2} + \frac{v\omega_2}{2c} \tag{17}$$

and

$$\phi = \frac{\phi_1 + \phi_2}{2} + \frac{\omega_2 d_0}{2c} \pm k\pi, \quad k = 0, 1, \tag{18}$$

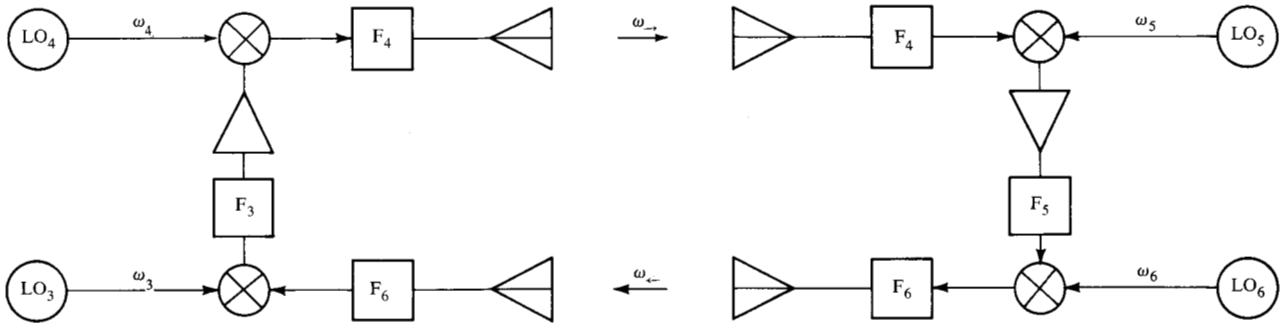

Case	Terminal type: Left (←)	Terminal type: Right (→)	Requirement for stable oscillation	Resulting frequency: $\omega_{\leftarrow}$	Resulting frequency: $\omega_{\rightarrow}$	Oscillator frequency for given link and intermediate frequencies: ω_3	ω_4	ω_5	ω_6
1	Shift up	Shift down	$\omega_3+\omega_5=\omega_4+\omega_6$ [a]	[b]	$\omega_{\leftarrow}-\omega_{\rightarrow}=\omega_3-\omega_4$	$\omega_{\leftarrow}-\omega_{if}$	$\omega_{\rightarrow}-\omega_{if}$	$\omega_{\rightarrow}-\omega_{if}$	$\omega_{\leftarrow}-\omega_{if}$
2	Invert up	Invert down	$\omega_3+\omega_4=\omega_5+\omega_6$ [a]	[b]	$\omega_{\leftarrow}+\omega_{\rightarrow}=\omega_3+\omega_4$	$\omega_{\leftarrow}-\omega_{if}$	$\omega_{\rightarrow}+\omega_{if}$	$\omega_{\rightarrow}-\omega_{if}$	$\omega_{\leftarrow}+\omega_{if}$
3	Shift up	Invert down	None	$\frac{\omega_4+\omega_5+\omega_6-\omega_3}{2}$	$\frac{\omega_3+\omega_5+\omega_6-\omega_4}{2}$	$\omega_{\leftarrow}-\omega_{if}$	$\omega_{\rightarrow}+\omega_{if}$	$\omega_{\rightarrow}-\omega_{if}$	$\omega_{\leftarrow}-\omega_{if}$
4	Invert up	Shift down	None	$\frac{\omega_3+\omega_4+\omega_5-\omega_6}{2}$	$\frac{\omega_3+\omega_4+\omega_6-\omega_5}{2}$	$\omega_{\leftarrow}-\omega_{if}$	$\omega_{\rightarrow}+\omega_{if}$	$\omega_{\rightarrow}-\omega_{if}$	$\omega_{\leftarrow}-\omega_{if}$

[a] Frequency discriminator and voltage control of one of the oscillators are required for a stable mode.
[b] Frequency is selected by filtering and limiting from among the multiple modes separated by π/t_d.

Figure 10 Systems using if amplification.

where d_0 is the initial distance between the terminals. Thus, with the single-inversion, single-shift system, there is a frequency at which oscillation occurs even with motion between the terminals. The local oscillators do not have to be adjusted to maintain a stable oscillation. As an example of the amount of carrier shift, consider the case of a desired nominal upper link frequency of 1000 MHz and a lower link frequency of 900 MHz. If the left hand terminal inverts, the oscillator frequency ω_1 would be 1900 MHz and ω_2 would be 100 MHz. Thus, relative motion requires the upper link frequency to shift by an amount equivalent to the one-way Doppler shift on $\omega_2/2$ or on 500 MHz.

For either the double-shift or double-inversion system, a similar procedure would show that the following two conditions must be met:

$$\omega=\frac{\omega_1}{2}+(\phi_2-\phi_1)\left(\frac{c+v}{2d_0}\right)\pm\frac{n\pi(c+v)}{d_0} \tag{19}$$

and

$$\omega_2=\frac{2\omega v}{c+v}+\omega_1\frac{c}{c+v}. \tag{20}$$

In this case, there are a number of possible frequencies of oscillation, each separated by

$$\Delta f=\frac{\Delta\omega}{2\pi}=\frac{c+v}{2d_0}. \tag{21}$$

It is also required that one of the local oscillator frequencies be adjusted from the nominal value $\omega_2=\omega_1$ by the amount

$$\Delta\omega_2\approx\frac{v}{c}(2\omega-\omega_1), \tag{22}$$

obtained from Eq. (20), where the approximation $v\ll c$ has been made.

Recall from Table 1 that the local oscillator frequency ω_1 for the double-shift case is small compared to ω. Hence, by Eq. (22), the Doppler shift is high. In contrast, the oscillator frequencies are high in the double-inversion case and the Doppler shifts are correspondingly very small.

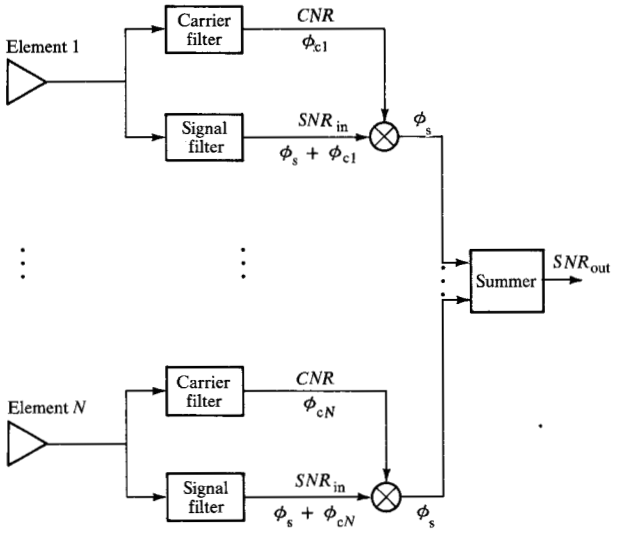

Figure 11 Demodulation method using pilot signal for dephasing.

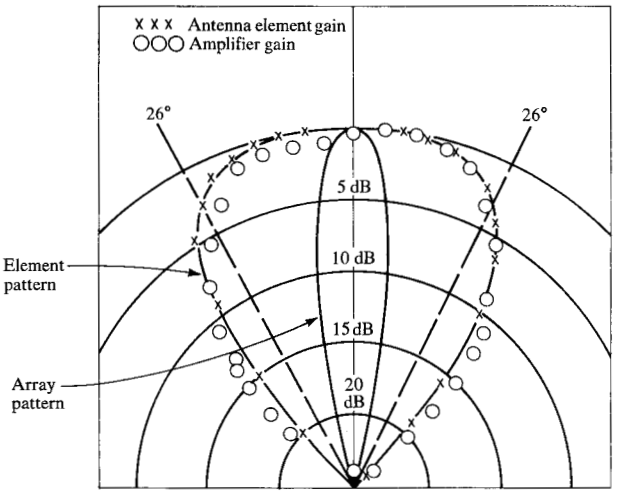

Figure 12 Experimentally determined amplifier gain increase required to initiate oscillation and antenna element gain decreases as functions of array orientation.

Modulation and demodulation

To realize the full antenna aperture gain on reception, the signals received at each array element must be summed in phase. The straightforward method of employing phase shifts between each element and the summing point requires a search procedure. A particularly useful approach, shown in Fig. 11, is due to Cutler, Tillotson and Kompfner [7]. In our use of the system, a pilot carrier frequency ω_c is built up between the two terminals. This carrier is filtered separately at each receiving element and is mixed with the separately filtered information-bearing signal at each element. If the percent of frequency separation between the carrier and the information signal is not too great, the lower sideband outputs of each mixer are of approximately the same phase and they can be summed. This process is essentially single sideband demodulation. The signal-to-noise ratio of the system output is approximately

$$SNR_{out} = N\left[\frac{(SNR_{in})(CNR)}{1 + SNR_{in} + CNR}\right], \tag{23}$$

where SNR_{in} is the input signal-to-noise ratio at each information channel, and CNR is the carrier-to-noise ratio at each mixer. The output signal-to-noise ratio is within 1 dB of its maximum value, $N(SNR_{in})$, if $CNR > 10$ and $CNR > 10\,SNR_{in}$.

It is desirable, of course, to limit the amount of power required for the carrier. The ratio of total required power to signal power can be shown to be

$$\frac{P_{total}}{P_{signal}} = 1 + N\left(\frac{B_c}{B_s}\right)\frac{CNR}{SNR_{out}}, \tag{24}$$

where B_c is the carrier filter bandwidth and B_s is the signal filter bandwidth. The carrier bandwidth required is a function of oscillator stabilities and Doppler shift uncertainty. A value between 100 and 1000 Hz is a reasonable estimate, unless carrier tracking loops are used. For wideband systems, the ratio given by Eq. (24) is close to one. Assume, as an example, $SNR_{out} = 100$, $CNR = 10$, $N = 1000$, $B_s = 10^6$ Hz and $B_c = 500$ Hz. This results in $P_{total}/P_{signal} = 1.05$, a negligible increase.

Other types of signal modulation can be used, as long as there is no spectrum spreading into the carrier channel. Accordingly a phase- or amplitude-modulated subcarrier may be used in the modulation channel and this signal may be time- or frequency-multiplexed.

Other modulation methods may be considered for the carrier as well. However, suppression of the carrier, which occurs in certain types of balanced modulation and with frequency modulation of specific modulation indices, must be avoided.

Non-engaged radiated power

The power level transmitted by the array in the absence of engagement of a station is of interest. This power, P_{to}, is given by

$$P_{to} = NG_eS_0B_c, \tag{25}$$

where B_c is the filter bandwidth used during startup (carrier bandwidth), G_e is the electronic power gain, and S_0 is the noise intensity (noise power per unit bandwidth). In terms of the loop gain G_ℓ this power is expressed by

$$P_{t0} = \frac{1}{N}\left(\frac{4\pi d}{g_a \lambda}\right)^2 (S_0 B_c G_\ell)^{\frac{1}{2}}, \tag{26}$$

where g_a is the gain of a single antenna element and λ is the carrier wavelength.

If both terminals have arrays of N elements and the signal outputs are coherently summed, the transmitter power required to provide a given SNR_{out} is given by

$$P_t = \left(\frac{4\pi d}{N\lambda g_a}\right)^2 (S_0 B_s) SNR_{out}. \tag{27}$$

The ratio of unengaged radiated power to the directed radiated power required for reception is therefore

$$\frac{P_{t0}}{P_t} = \frac{N}{SNR_{out}}\left(\frac{B_c}{B_s}\right) G_\ell^{\frac{1}{2}}. \tag{28}$$

This noise power is distributed over the field of view of the array, which is the beamwidth of the individual antenna elements. It can be compared to the power that is transmitted over the same beamwidth by a system using only one element at each terminal and having the same output signal-to-noise ratio. This power, which can be considered as noise or interference to other users, is given by

$$P_{ta} = N^2 P_t. \tag{29}$$

Therefore,

$$\frac{P_{t0}}{P_{ta}} = \frac{G_\ell^{\frac{1}{2}}}{N(SNR_{out})}\left(\frac{B_c}{B_s}\right), \tag{30}$$

the value of which can be considerably less than one. For example, for $N = 100$, $SNR_{out} = 100$, $B_c/B_s = 0.1$ and a loop gain of two, the value is $\sqrt{2} \times 10^{-5}$.

Experimental results

The self-directional principle of communication has been demonstrated with four-channel arrays retrodirective in the horizontal plane, operating with link frequencies of 410 and 480 MHz. The distance between terminals was 750 feet (230 m).

With the system operating at full array gain, the amplifier gain was reduced to the level at which oscillation was extinguished. Then an experiment was conducted in which the amplifier gain was raised from a level insufficient to support oscillation to the level at which oscillation began. The fact that the gain required to initiate oscillation was the same as that at which existing oscillation became extinguished showed that the full array gain was available under all conditions.

The experimentally determined increase in amplifier gain required to initiate oscillation at angles off broadside is plotted in Fig. 12. Also plotted is the decrease in element gain that occurred when the array was steered off broadside. These data were determined by forming the products of the element patterns for elements operating at 410 and 480 MHz. As seen in the plot, the decrease in element gain as a function of angle is offset by the increase in amplifier gain required to initiate oscillation. The half-power (−3 dB) beamwidth of the antenna element is seen to be 52 degrees in the horizontal plane and is equal to the array field of view.

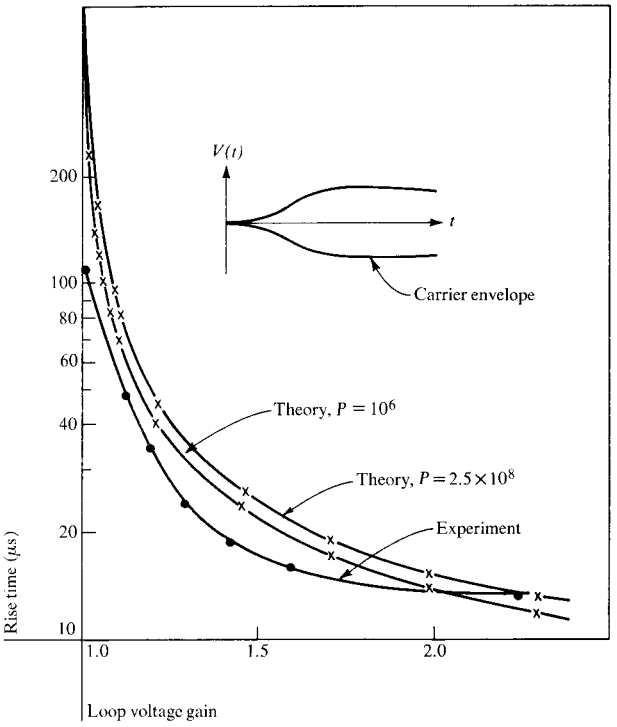

Figure 13 Comparison of theoretical and experimentally determined oscillation build-up time as function of loop voltage gain.

Measurement of the array gain confirmed that the system beam is truly a narrow phased-array pattern in the horizontal plane. The half-power beamwidth of the array pattern was determined to be 10 degrees in the retrodirective plane.

Oscillation build-up time was also measured. The experimental results, compared with theoretical predictions, are shown in Fig. 13.

The form of the oscillation modes was observed for a single-channel delay line system for various values of loop gain. These results are shown in Fig. 14. The mode structure exhibits the periodic form predicted in the theoretical analysis and shows the process of single-mode selection as loop gain is increased. A carrier-to-noise ratio of greater than 40 dB was obtained when the loop gain was high enough to select a single mode of oscillation.

Other experiments verified system operation at L-band frequencies using both nine- and twelve-element arrays. Carrier build-up, operation of a conformal array, and

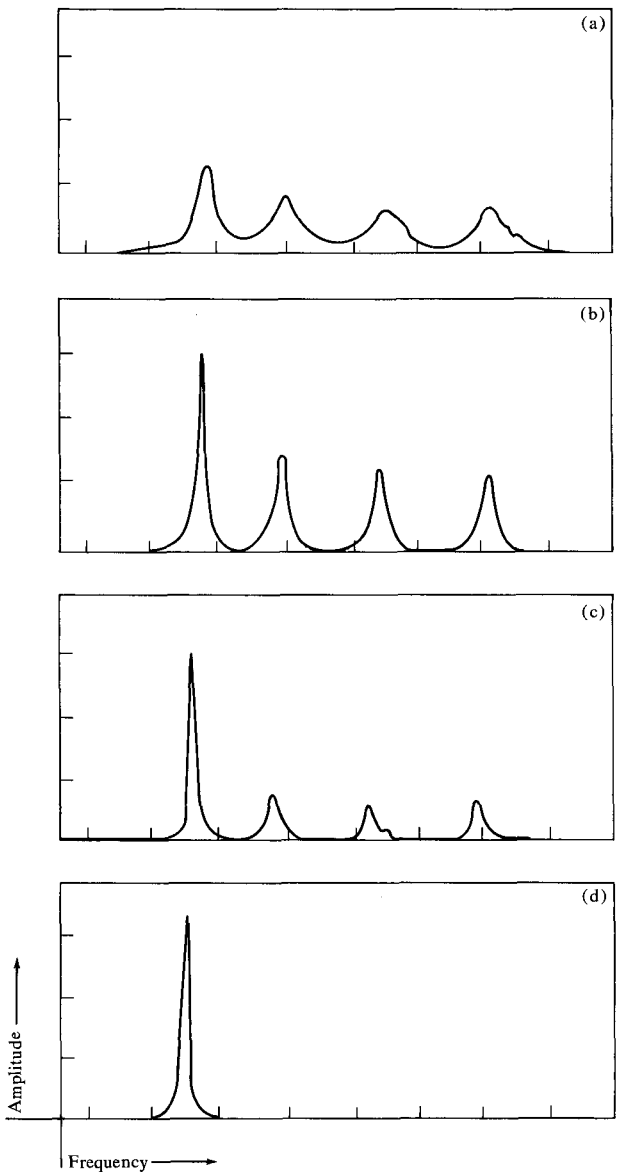

Figure 14 Mode spectra observed for a single channel delay line system at 480 MHz. (a) Loop gain = −7.0 dB, (b) −3.5 dB, (c) −1.5 dB, (d) 0 dB.

single inversion have been experimentally demonstrated. Multidirectional performance was also exhibited by providing simultaneous transmission and reception in two directions.

Summary

We have shown by analysis and verified by experiment that two retrodirective arrays within each others' field of view will, starting from thermal noise, develop an oscillating signal around the loop formed by the arrays. This signal takes the spatial form of a directed beam from one terminal to another. Signal build-up requires that the loop gain be greater than one. This loop gain includes the full array gain of each terminal, that is, the array gain with coherent excitation. The operability of the array gain during the build-up period was validated by experiment.

The build-up time, which is a function of the loop gain, is of the order of 15 to 30 loop one-way trips.

To allow reception and transmission at different frequencies, frequency conversion can be used in each terminal. The received signal in each terminal can be translated in frequency either with or without inversion. A system using frequency inversion in only one terminal has the desirable feature of not requiring synchronization between the oscillators in the two terminals or requiring a frequency control circuit. The resulting frequency in this system is independent of the distance between the terminals and a stable mode of oscillation occurs even with relative motion between the two terminals.

With or without frequency translation in the terminals, the oscillating signal during the linear build-up phase may consist of many modes, depending upon the ratio of loop bandwidth and time delay. When limiting occurs, the mode with the largest amplitude will, under most circumstances, suppress the other modes. In the single-inversion system all modes except one, designated the main mode, occur in pairs. These pairs are related in phase such that they appear as amplitude modulation on the main mode and are therefore rapidly suppressed when limiting occurs.

In all these systems the oscillating signal can be used as a carrier that can be modulated with an information signal, thus providing the basis for a self-directional communication system.

Although this system radiates noise throughout the field of view of the arrays, the power level of this noise for most applications would be several orders of magnitude less than the power radiated using an omnidirectional system.

Acknowledgments

The authors thank Maurice Karnaugh for providing much helpful guidance and analytical insight and Sylvester Miniter, who was instrumental in the experimental demonstration of the system. Part of this work was done under contract numbers AF33(615)-3552 and F33615-67-C-1644, which were sponsored by the Department of Defense Advanced Research Projects Agency and monitored by the Air Force Avionics Laboratory.

Appendix: Analysis of oscillation build-up

Figure A1 shows a diagram of the system configuration displayed in Fig. 2. The voltage inputs n_{11}, n_{12}, n_{21}, and n_{22} are thermal noise sources. They do not include noise received from the opposite terminal or other external

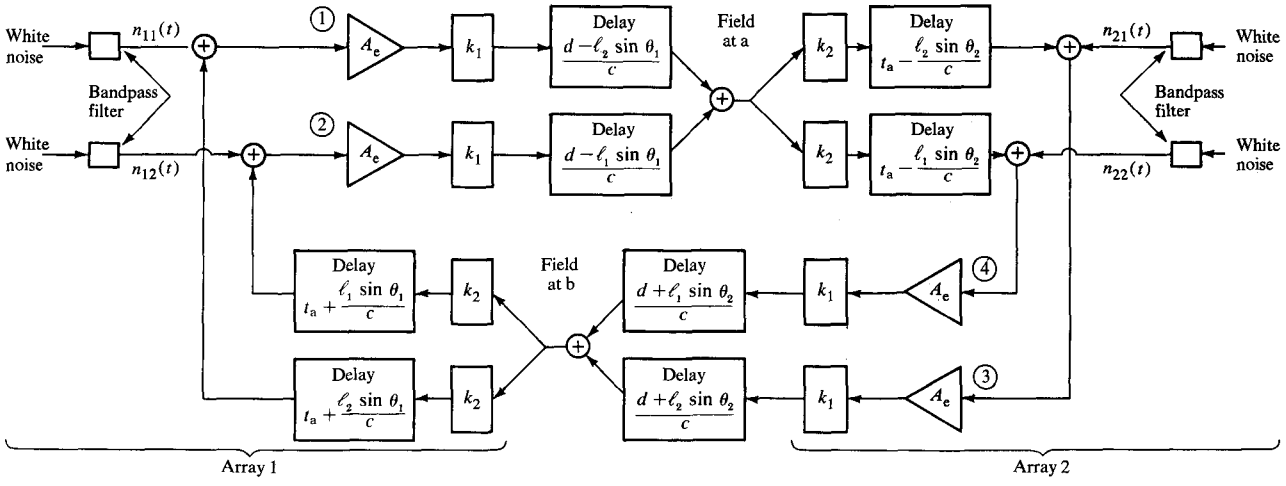

Figure A1 Schematic diagram for analysis of system shown in Fig. 2.

sources of noise. Each signal emanating from Array 1 produces a field at point a of Array 2. Similarly, signals from Array 2 produce a field at point b of Array 1, where a and b are separated by a distance d.

The boxes labeled k_1 represent the individual transmitting antenna elements as well as space attenuation. This factor is

$$k_1 \equiv [g_a/4\pi d^2]^{\frac{1}{2}}, \tag{A1}$$

where g_a is the power gain of a single antenna element and $1/4\pi d^2$ is the power attenuation resulting from signal travel over a distance d.

The boxes labeled k_2 represent the aperture of a single receiving element. The aperture is defined by

$$k_2^2 \equiv \frac{\lambda^2}{4\pi} g_a, \tag{A2}$$

where λ is the signal wavelength.

The time it takes for a signal to travel the electrical path from a receiving element to its corresponding transmitting element in the same array is denoted in the diagram by the delay factor t_a. Because Arrays 1 and 2 may be tilted from broadside by angles θ_1 and θ_2, respectively, the actual internal delays and transmission times are calculated from the expressions shown in the "delay" boxes of Fig. A1, where the distances from points a and b to the array elements have been taken into account. Note that the total loop delay from a given point in an array through any channel in the opposite array and back to the point of reference is given by $2[(d/c) + t_a] \equiv 2t_d$, where t_d is one-half the total loop transit time and c is the speed of signal propagation.

In the analysis that follows, we derive the power spectral density of the signal at the input to one of the array amplifiers. This expression allows us to see how the spectrum changes during the build-up period before limiting occurs in the system. The density function is computed from the autocorrelation function of the amplifier input.

Although the autocorrelation function changes with time, intervals exist during which it is independent of time. During these time-independent intervals we can assume that the amplifier input is a stationary random process. The power spectral density can then be calculated by taking the Fourier transform of the autocorrelation function [8, 9].

The amplifier input is considered to be the output $y(t)$ of a linear system having an impulse response function $h(t)$. The system input $x(t)$ is assumed to be a stationary random process applied at $t = 0$. Under these conditions the output autocorrelation function for all t_1 and t_2 greater than zero is given by

$$R_{yy}(t_1, t_2) = R_{xy}(t_1, t_2)*h(t_1). \tag{A3}$$

where * denotes the convolution integral.

The cross-correlation function is computed from

$$R_{xy}(t_1, t_2) = R_{xx}(t_1, t_2)*h(t_1). \tag{A4}$$

If a stationary random process with autocorrelation $R(\tau)$ is applied to a linear system at $t = 0$, the input autocorrelation is given by

$$R_{xx}(t_1, t_2) = \begin{cases} R(t_1 - t_2) \text{ for } t_1, t_2 > 0; \\ 0, \text{ otherwise.} \end{cases} \tag{A5}$$

Setting $t_1 = t + \tau$ and $t_2 = t$, (A5) gives $R_{xx}(t + \tau, t) = R(\tau)$ when t and $t + \tau$ are greater than zero, and is zero otherwise.

If the thermal noise inputs are assumed to be narrowband noise, i.e., the result of passing white noise through an ideal filter with center frequency ω_c and bandwidth

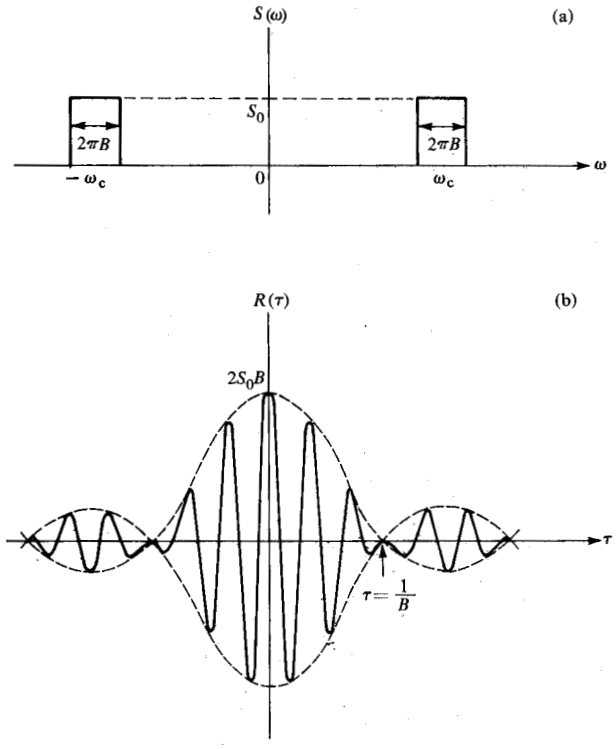

Figure A2 (a) Power spectrum and (b) autocorrelation function of band-limited white noise.

$2\pi B$, they each have a spectrum $S(\omega)$ as shown in Fig. A2(a), where

$$S(\omega) = \begin{cases} S_0 \text{ for } |\omega_c - \pi B| \leq \omega \leq |\omega_c + \pi B|; \\ 0, \text{ otherwise.} \end{cases} \tag{A6}$$

The autocorrelation of these inputs is

$$R(\tau) = \frac{2S_0 \sin \pi B\tau}{\pi\tau} \cos \omega_c\tau, \tag{A7}$$

which is plotted in Fig. A2(b).

With Point 1 in Fig. A1 as the output, the impulse responses from Points 1, 2, 3, and 4 are, respectively,

$$h_1(t) = \delta(t) + \frac{1}{N}\sum_{n=1}^{\infty} A^{2n}\delta(t - 2nt_d); \tag{A8}$$

$$h_2(t) = \frac{1}{N}\sum_{n=1}^{\infty} A^{2n}\delta\left[t - 2nt_d - \frac{(\ell_2 - \ell_1)\sin\theta_1}{c}\right]; \tag{A9}$$

$$h_3(t) = \frac{1}{N}\sum_{n=0}^{\infty} A^{2n+1}\delta\left[t - (2n+1)t_d - \frac{2\ell_2}{c}(\sin\theta_1 + \sin\theta_2)\right]; \tag{A10}$$

$$h_4(t) = \frac{1}{N}\sum_{n=0}^{\infty} A^{2n+1}\delta\left[t - (2n+1)t_d - \frac{\ell_1 \sin\theta_2 + \ell_2 \sin\theta_1}{c}\right], \tag{A11}$$

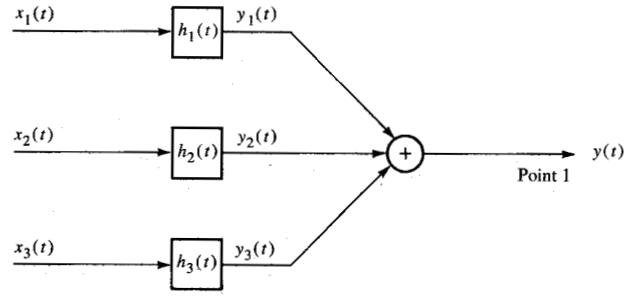

Figure A3 Diagram used for analysis of input to a single amplifier.

where $\delta(t)$ is the Dirac delta function, $A \equiv NA_e k_1 k_2 = Ng_a A_e \lambda/4\pi$, A_e is the electronic gain, and n is the number of one-way trips between the terminals.

The last three impulse responses can be simplified by deleting the constant delay factors. This is equivalent to assuming that the input noise sources appear at different points in each channel. Since these noise sources are independent, this assumption can have no significant effect upon the results. With this assumption, the model shown in Fig. A3 can be adopted for two identical arrays of N elements each. We define the input $x_1(t)$ as n_{11}, the input x_2 as the sum of all other thermal noise inputs to Array 1, and input x_3 as the sum of all thermal noise inputs to Array 2. The autocorrelation functions of x_1, x_2, and x_3 are, respectively, $R(\tau)$, $(N-1)R(\tau)$, and $NR(\tau)$, where N is the number of antenna elements in each array.

The impulse responses to x_1, x_2, and x_3 are, respectively,

$$h_1(t) = \delta(t) + \frac{1}{N}\sum_{n=1}^{\infty} A^{2n}\delta(t - 2nt_d), \tag{A12}$$

$$h_2(t) = \frac{1}{N}\sum_{n=1}^{\infty} A^{2n}\delta(t - 2nt_d), \text{ and} \tag{A13}$$

$$h_3(t) = \frac{1}{N}\sum_{n=0}^{\infty} A^{2n+1}\delta[t - (2n+1)t_d]. \tag{A14}$$

We can now use Eqs. (A3) and (A4) to calculate the autocorrelation functions:

$$\begin{aligned} R_{y_1y_1}(t+\tau, t) &= R(\tau)U(t+\tau)U(t) \\ &+ \frac{1}{N}\sum_{n=1}^{\infty} A^{2n}R(\tau + 2nt_d)U(t+\tau)U(t - 2nt_d) \\ &+ \frac{1}{N}\sum_{n=1}^{\infty} A^{2n}R(\tau - 2nt_d)U(t+\tau-2nt_d)U(t) \\ &+ \frac{1}{N^2}\sum_{m=1}^{\infty} A^{2m}\sum_{n=1}^{\infty} A^{2n}R[\tau + 2(m-n)t_d] \\ &\times U(t+\tau-2nt_d)U(t-2mt_d); \end{aligned} \tag{A15}$$

$$R_{y_2y_2}(t+\tau, t) = \left(\frac{N-1}{N^2}\right) \sum_{m=1}^{\infty} A^{2m}$$

$$\times \sum_{n=1}^{\infty} A^{2n} R[\tau + 2(m-n)t_d]$$

$$\times U(t+\tau-2nt_d)U(t-2mt_d); \quad \text{(A16)}$$

$$R_{y_3y_3}(t+\tau, t) = \frac{1}{N} \sum_{m=0}^{\infty} A^{2m+1}$$

$$\times \sum_{n=0}^{\infty} A^{2n+1} R[\tau + 2(m-n)t_d]$$

$$\times U[t+\tau-(2n+1)t_d]U[t-(2m+1)t_d], \quad \text{(A17)}$$

where $U(t-a)$ is the unit step function; i.e., $U(t-a) = 1$ if $t \geq a$, and is zero otherwise.

As seen in Fig. A2(b), the envelope of $R(\tau)$ decreases with $|\tau|$ and is small for $|\tau| > 2/B$. Therefore, a term such as $R(\tau)U(t+\tau)U(t)$ is approximately independent of time as long as $t > 2/B$. Thus, the autocorrelations above can be considered independent of time during the intervals $t_d - 2/B = (n+1)t_d - (nt_d + 2/B)$ if $B > 2/t_d$. (If this inequality is not satisfied, oscillations will still build up but at a slower rate than that given by the subsequent derivation.)

The sum of Eqs. (A15)–(A17) gives the following autocorrelation function for the time-independent intervals:

$$R_{yy}(\tau) = R(\tau) + \frac{1}{N} \sum_{j=1}^{n/2} A^{2j}[R(\tau + 2jt_d) + R(\tau - 2jt_d)]$$

$$+ \frac{1}{N} \sum_{k=1}^{n/2} A^{2k} \sum_{j=1}^{n/2} A^{2j} R[\tau + 2(k-j)t_d]$$

$$+ \frac{1}{N} \sum_{k=0}^{(n/2)-1} A^{2k+1} \sum_{j=0}^{(n/2)-1} A^{2j+1} R[\tau + 2(k-j)t_d],$$

for even n. (A18)

If an autocorrelation function is independent of time, the power spectral density can be obtained by taking its Fourier transform [8, 9]. The Fourier transform of Eq. (A18) is denoted by $S_n(\omega)$ and we obtain

$$\frac{S_n(\omega)}{S(\omega)} = 1 + \frac{A^2}{N}(1 + A^2 + A^4 + \cdots + A^{2n-2})$$

$$+ \frac{A^2}{N}(1 + A^2 + A^4 + \cdots + A^{2n-4}) \cos 2\omega t_d$$

$$+ \frac{A^4}{N}(1 + A^2 + A^4 + \cdots + A^{2n-8}) \cos 4\omega t_d$$

$$\vdots$$

$$+ \frac{A^n}{N} \cos n\omega t_d, \quad \text{(A19)}$$

or, in a more useful form for $A \neq 1$,

$$S_n(\omega)/S(\omega) = 1 + \{A^2[1 - A^2 + A^4 - A^{2n+4}$$

$$+ (1 - 2A^2 + A^{2n+2}) \cos 2\omega t_d]$$

$$+ A^{n+2}(A^2 - 1)[\cos n\omega t_d + \cos(n+2)\omega t_d]\}$$

$$\div N(1 - A^2)(1 + A^4 - 2A^2 \cos 2\omega t_d). \quad \text{(A20)}$$

The loop power gain with coherent excitation of the arrays is given by

$$G_\ell = (Ng_a A_e \lambda / 4\pi)^4 \quad \text{(A21)}$$

and, comparing this with the definition of A, we have

$$G_\ell = A^4. \quad \text{(A22)}$$

Equation (A20) shows that the power spectrum increases continuously with n as long as A is greater than one. From Eq. (A22) this is equivalent to oscillation build-up as long as the loop gain (including coherent excitation of both arrays) is greater than one.

References

1. Special issue on active and adaptive antennas, *IEEE Trans. Antennas and Propagation* **AP-12,** No. 2 (1964).
2. E. L. Gruenberg, *U.S. Patent No. 3,757,335.*
3. L. Espenshied, *U.S. Patent No. 2,467,299.*
4. L. Van Atta, *U.S. Patent No. 2,908,002.*
5. H. P. Raabe, *U.S. Patent No. 3,757,334.*
6. W. A. Edson, "Frequency Memory in Multi-mode Oscillators," *IRE Trans. Circuit Theory* **CT-2,** 58 (1955).
7. C. C. Cutler, R. Kompfner and L. C. Tillotson, "A Self-Steering Array Repeater," *Bell Syst. Tech. J.* **42,** 2013 (1963).
8. W. B. Davenport, Jr. and W. L. Root, *An Introduction to the Theory of Random Signals and Noise,* McGraw-Hill Book Co., Inc., New York, 1965.
9. A. Papoulis, *Probability, Random Variables and Stochastic Processes,* McGraw-Hill Book Co., Inc., New York, 1965.

Received March 21, 1973; revised September 8, 1973

E. L. Gruenberg was with the IBM Federal Systems Division at the Federal Systems Center in Morris Plains, New Jersey 07950; his current address is 6040 Boulevard East, West New York, New Jersey 07093. H. Raabe is at the FSD Electronics Systems Center in Manassas, Virginia 22110; and C. T. Tsitsera is at the FSD Electronics Systems Center in Owego, New York 13827.